

RSC Advances



This is an *Accepted Manuscript*, which has been through the Royal Society of Chemistry peer review process and has been accepted for publication.

Accepted Manuscripts are published online shortly after acceptance, before technical editing, formatting and proof reading. Using this free service, authors can make their results available to the community, in citable form, before we publish the edited article. This *Accepted Manuscript* will be replaced by the edited, formatted and paginated article as soon as this is available.

You can find more information about *Accepted Manuscripts* in the [Information for Authors](#).

Please note that technical editing may introduce minor changes to the text and/or graphics, which may alter content. The journal's standard [Terms & Conditions](#) and the [Ethical guidelines](#) still apply. In no event shall the Royal Society of Chemistry be held responsible for any errors or omissions in this *Accepted Manuscript* or any consequences arising from the use of any information it contains.

Selective Fluorescence Sensing of Salicylic Acids Using a Simple Pyrenesulfonamide Receptor

Ashwani Kumar,^a Manik Kumer Ghosh,^b Cheol-Ho Choi,^b and Hong-Seok Kim^{a*}

^a *School of Applied Chemical Engineering, Department of Applied Chemistry, Kyungpook National University, Daegu 702-701, Republic of Korea*

^b *Department of Chemistry, and Green-Nano Materials Research Center, College of Natural Sciences, Kyungpook National University, Daegu 702-701, Republic of Korea*

* *Corresponding author: Tel.: +82 53 9505588; Fax: +82 53 9506594*

E-mail address: kimhs@knu.ac.kr

Abstract

Pyrenesulfonamide and pyreneamide probes (**2–5**) were synthesized, and they were used in the sensing of salicylic acid derivatives. The ability of **3** to sense various salicylic acid derivatives was examined by UV-visible, fluorescence, and NMR spectroscopy; it was further supported by DFT calculations. The sensing of salicylic acid derivatives resulted in a significant quenching of the pyrene monomer emission. Among the tested salicylic acid derivatives, probe **3** exhibited the highest binding constant with 3,5-dinitrosalicylic acid ($K_a = 2.65 \times 10^5 \text{ M}^{-1}$, measured at a 1:1 molar ratio in EtOH).

Keywords: Fluorogenic receptor; Pyrenesulfonamide, 3-Aminopropylimidazole, Salicylic acid derivatives.

1. Introduction

Because of the significant roles that carboxylic acids play in metabolism/biology, there is a growing interest in being able to sense them.¹ Carboxylic acids find several applications in various fields, such as the food industry,² medical diagnosis,³ environmental monitoring,⁴ and process control.⁵ A variety of probes with different binding sites, such as amines (having N-H groups as hydrogen-bonding sites),⁶ quaternary ammonium/imidazolium salts (having positive charges for ionic interactions in addition to hydrogen bonding),⁷ ureas,⁸ amides,⁹ α -aminopyridines/ α -amidopyridines¹⁰ α,α' -diaminopyridines/ α,α' -diamidopyridines, and diamides¹¹ (having two hydrogen-bonding sites in the same probe), linked to different fluorophores/heterocycles, have been used for the sensing of carboxylic acids.¹² We focused our research efforts on the sensing of aromatic (instead of aliphatic) carboxylic acids.¹³

In the last two decades, sulfonamides appended with various chromophores/fluorophores have found potential applications in the sensing of different analytes, such as metal ions, anions and neutral molecules.¹⁴ Recently, among different fluorophores, pyrenesulfonamides conjugated with various amino acids have been used for metal-ion sensing,¹⁵ and gluconolinked pyrenesulfonamides were found to behave as gelators in tetrahydrofuran–water mixtures.¹⁶ One of the butterfly-shaped cholesterol-conjugated pyrenesulfonamide dipodes exhibits ratiometric excimer emission: an increase in the concentration of water in solvents such as ethanol, methanol, and acetonitrile leads to a decrease in monomer emission.¹⁷

Recently, pyrene-appended aminopropylimidazole probe **1** was reported to be an effective sensor for salicylic acid.^{13b} Probe **1**, having an imidazole ring and an amino group (N-H) as hydrogen-bonding motifs and a pyrene fluorophore for the π - π interactions, was designed based on hydrogen-bonding complementarity between the host and guest and on an increase in the intensities of monomer emission bands. Because of the methylene (CH₂) unit between the amino group and the pyrene unit, the lone pair of the amino nitrogen is not conjugated

with the aromatic core of the pyrene unit, which results in a weak emission intensity of probe **1**. Upon the addition of various aromatic carboxylic acids (ACAs) to a solution of probe **1** ($3\ \mu\text{M}$ in EtOH), a selective “switch on” of the fluorescence emission intensity of the pyrene monomer takes place. This occurs with salicylic acid (SA) and SA derivatives that have electron-withdrawing groups, such as 5-nitrosalicylic acid (5-NSA) and 5-iodosalicylic acid (5-ISA). It is caused by the restricted rotation of the benzene ring in SA and its derivatives, because of intramolecular hydrogen bonding between the phenolic O-H group and the neighboring C=O group (Fig. 1).^{13b} The degree of emission enhancement is dependent on the substituent and on the orientation of the benzoic acid (BA) hydroxyl group.

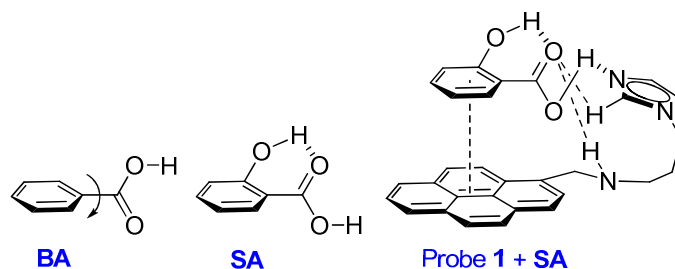


Fig. 1: Free rotation of the carboxylic acid group is possible in BA, free rotation of the carboxylic acid group is prohibited in SA, and scheme of complexation of probe **1** with SA.

In the case of imidazole receptors, the imidazole C2-H group participates in hydrogen bonding with anions.¹⁸ Keeping in mind the active roles of the sulfonamide N-H and imidazole C2-H groups and the good fluorescence monomer/excimer emission of pyrene, we designed very simple pyrenesulfonamide/pyreneamide probes **2-5** for the detection of SA derivatives (Fig. 2). This is the first report in which pyrenesulfonamides are used for the sensing of SA derivatives.

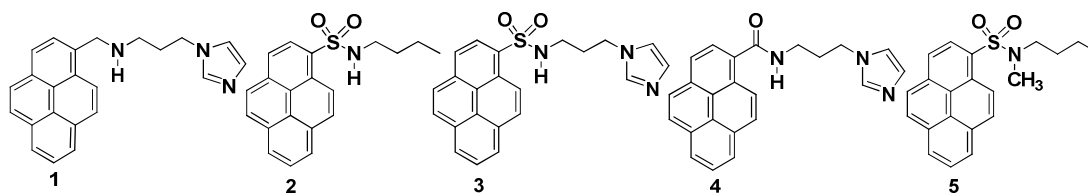
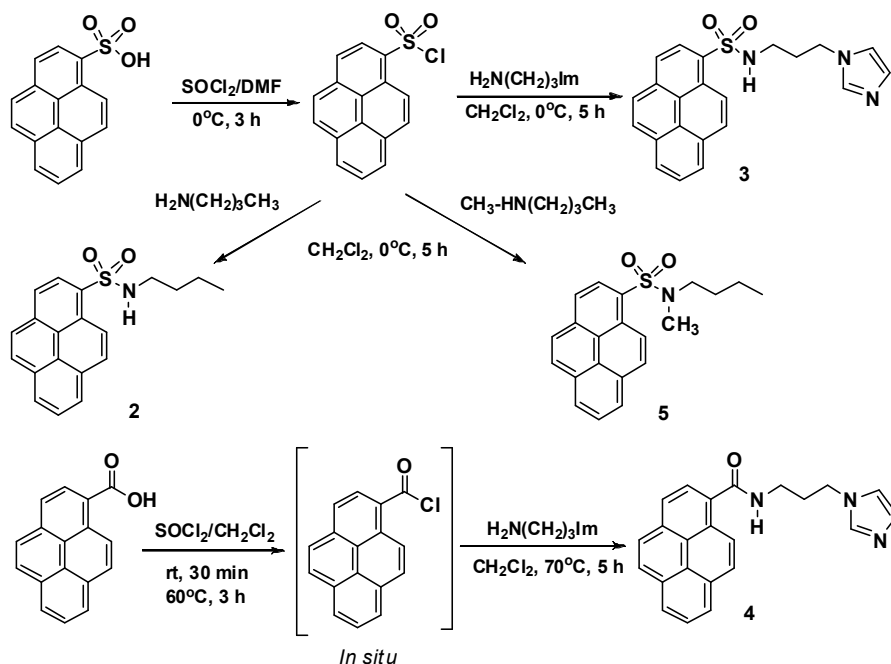


Fig. 2: Structures of pyrenesulfonamide and pyreneamide probes 1–5.

2. Results and Discussion

Probes 2–5 are easily synthesized in good yields, in a single step, by the reaction of either pyrenesulfonyl chloride or 1-pyrenecarboxylic acid chloride with amines (Scheme 1). The structures of 2–5 were confirmed by ¹H and ¹³C NMR spectroscopy and by FAB mass spectrometry (see ESI). The ¹H NMR spectrum of 2 in CDCl₃ shows four signals due to aliphatic protons, at δ 0.73 (triplet for CH₃), δ 1.17–1.22 (multiplet for CH₂), δ 1.35–1.39 (multiplet for CH₂), and δ 2.94 (triplet for CH₂), and a broad singlet at δ 4.73 for the N-H group, in addition to other signals due to aromatic protons. The mass spectrum of 2 clearly shows a molecular ion peak at *m/z* 337.1141 (M⁺). Similarly, the ¹H NMR spectrum of probe 3 in DMSO-*d*₆ shows three signals for the propyl CH₂ groups (two multiplets at δ 1.68–1.72 and δ 2.73–2.75, one triplet at δ 3.84) and three singlets for the imidazole protons (at δ 6.72, δ 6.85, and δ 7.36 for H-b, H-c, and H-a, respectively). The ¹³C NMR spectrum of probe 3 shows a signal for the imidazole C-2 at δ 137.4. The mass spectrum of probe 3 clearly shows a molecular ion peak at *m/z* 390.1273 ([M + H]⁺). The ¹³C NMR spectrum of 4 clearly shows a peak due to the C=O group at δ 169.41. ¹H and ¹³C NMR spectra of 5 show singlets at δ 2.80 and δ 34.54, respectively, for the NCH₃ group. These spectral features indicate the successful formation of these probes.



Scheme 1. Synthesis of pyrenesulfonamides **2**, **3**, and **5**, and of pyreneamide **4**.

The UV-visible absorption spectrum of probe **2** exhibits typical pyrene absorption maxima at $\lambda_{\text{max}} = 322, 336,$ and 350 nm in EtOH. Upon excitation of **2** ($1 \mu\text{M}$ in EtOH) at 336 nm, it exhibits fluorescence emission maxima at $379, 398,$ and 420 nm with a high quantum yield ($\Phi = 0.213$); this stands in contrast to probe **1**, which has a weak fluorescence emission. In case of probe **2**, the extended conjugation between the sulfonamide nitrogen and the pyrene unit leads to easy charge transfer and a high quantum yield. Probe **3** has the highest quantum yield ($\Phi = 0.232$) among these probes. Probe **4** also has a good quantum yield ($\Phi = 0.160$), whereas probe **5** (having a NCH_3 instead of a NH functionality in the sulfonamide) has the lowest quantum yield ($\Phi = 0.045$); this clearly signifies the role of the sulfonamide NH functionality (Fig. 3). Upon the addition of 10 equiv of an ACA to a solution of probe **2**, the fluorescence emission intensity of **2** is quenched selectively with salicylic acid derivatives. The extent of quenching is $>95\%$ with 3,5-DNA, 50% with 5-NSA, and 20% with 5-ISA,

while other ACAs do not show any significant changes in the emission intensity of probe **2** (Figs. 4).

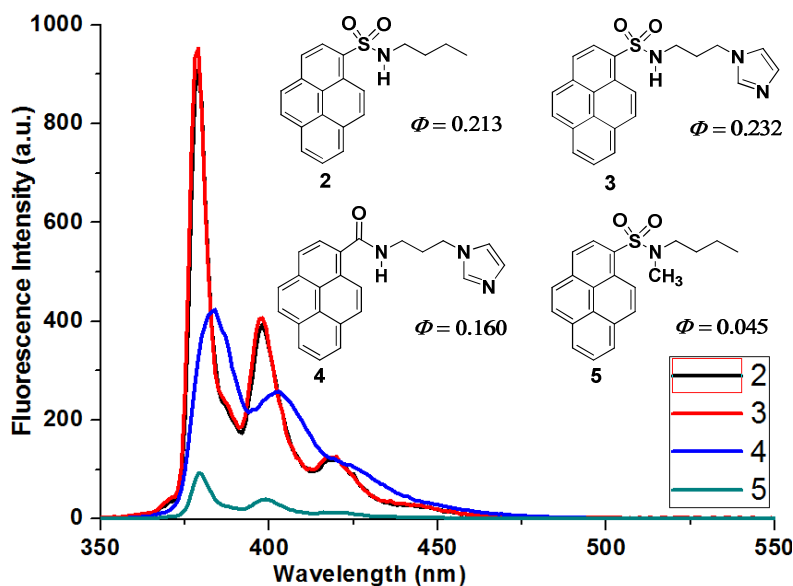


Fig. 3: Fluorescence emission intensities of probes **2–5** (1 μM in EtOH, $\lambda_{\text{ex}} = 336 \text{ nm}$).

The degree of quenching of the fluorescence emission intensities of the probes is dependent on the substituent and on the orientation of the hydroxyl group of benzoic acid (BA). The 2-hydroxyl group of SA forms an intramolecular hydrogen bond with the C=O group, which restricts the rotation of the carboxylic acid group. The combined effects of the intermolecular hydrogen bonding ((a) S=O---H-O, (b) SO₂N-H---O=C) and the intramolecular hydrogen bonding ((c) O-H---O=C) between probe **2** and SA (or SA derivatives) bring two aromatic moieties close enough to each other to affect the fluorescence emission intensity of probe **2**. The degree of the decrease in the fluorescence monomer emission intensity of probe **2** clearly shows that 3,5-DNSA interacts more strongly with probe **2** than 5-NSA (which, in turn, interacts more strongly than 5-ISA). This demonstrates that the degree of quenching of the fluorescence emission intensity depends on the electron-withdrawing nature of the aromatic substituents in SA derivatives. We attribute this to the

fact that the aromatic rings of these SA derivatives are electron deficient; they can accept electron charge from the pyrenesulfonamide probe **2**. In the absence of these SA derivatives, probe **2** is highly fluorescent because no charge transfer will occur, whereas in the presence of 3,5-DNSA, 5-NSA, or 5-ISA, the charge transfer occurs easily, resulting in the quenching of the fluorescence emission intensity.

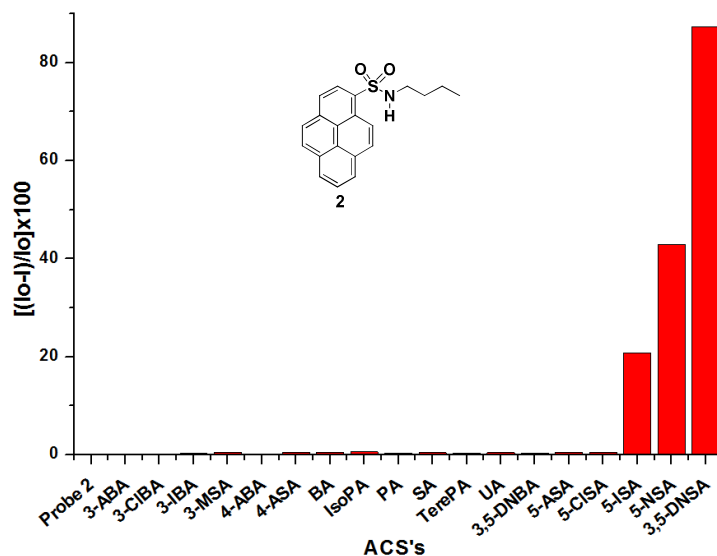


Fig. 4: Bar diagram of the relative fluorescence intensities of probe **2** (1 μ M in EtOH, λ_{ex} = 336 nm, λ_{em} = 379 nm) in the presence of various ACS's.

Although molecules similar to salicylic acid (such as salicylaldehyde, salicylamide, salicylhydroxamic acid, anthranilic acid, picolinic acid, and indole-2-carboxylic acid (Fig. SI-1)) were also tested with probe **2**, they did not cause any changes in the emission intensity of probe **2**. This observation indicates that an α -phenolic OH is essential for the restriction of the rotation of the C(O)OH group. Electron-withdrawing groups such as nitro and iodo groups make the aromatic ring more electron deficient, so that the C(O)OH hydroxyl groups in 3,5-DNSA, 5-NSA, and 5-ISA act as hydrogen donors (hydrogen-bonding units) toward the sulfonamide oxygen. The C(O)OH carbonyl oxygens act as hydrogen acceptors (hydrogen-

bonding units) toward the sulfonamide N-H functionality of probe **2**. The formation of intermolecular hydrogen bonds is not very effective when picolinic acid, indole-2-carboxylic acid, anthranilic acid, salicylaldehyde, salicylamide, and salicylhydroxamic acid are used.

To explore the binding constants for the binding of probe **2** with salicylic acid derivatives, we carried out fluorescence titrations on probe **2**. Upon the gradual addition of 3,5-DNSA to a solution of probe **2**, the fluorescence emission intensity decreases until the emission is eventually quenched completely (Figs. SI 2 and SI-3). The fluorescence titration shows that a 1:1 complex between probe **2** and 3,5-DNSA is formed with a high association constant ($K_a = 2.83 \times 10^4 \text{ M}^{-1}$; see Table 1). Similarly, fluorescence titrations of probe **2** with 5-NSA and 5-ISA show the formation of 1:1 complexes as well, with association constants of $9.07 \times 10^3 \text{ M}^{-1}$ and $5.32 \times 10^3 \text{ M}^{-1}$, respectively, along with quenching of fluorescence emission intensity. The association constants for the complexation of 5-NSA and 5-ISA to probe **2** are approximately ten times lower than those measured for probe **1**. On the other hand, the “switch off” of the fluorescence emission observed for probe **2** is the opposite of the “switch on” phenomenon observed for probe **1** (upon complexation with 5-NSA and 5-ISA).

To investigate the effect of the C2-H group of an imidazole ring, we designed and synthesized probe **3**, having acidic sulfonamide N-H functionality for hydrogen bonding and C2-H of an imidazole ring as an additional hydrogen bonding motif. Upon excitation of probe **3** (1 μM in EtOH) at 336 nm, the emission spectrum shows strong pyrene monomer fluorescence emission peaks at $\lambda_{\text{max}} = 379, 398, \text{ and } 420 \text{ nm}$ with a high quantum yield ($\Phi = 0.232$). Upon the addition of ACAs to the solution of probe **3**, it exhibits behavior similar to probe **2**, i.e., the degree of quenching of the pyrene monomer emission is 3,5-DNSA \gg 5-NSA $>$ 5-ISA (Fig. SI-4). Upon the gradual addition of 3,5-DNSA to a solution of probe **3**, the fluorescence emission intensity decreases with each addition and the emission is

eventually quenched completely (Fig. 5). The fluorescence titration shows the formation of a 1:1 complex between **3** and 3,5-DNSA with a high association constant ($K_a = 2.66 \times 10^5 \text{ M}^{-1}$).

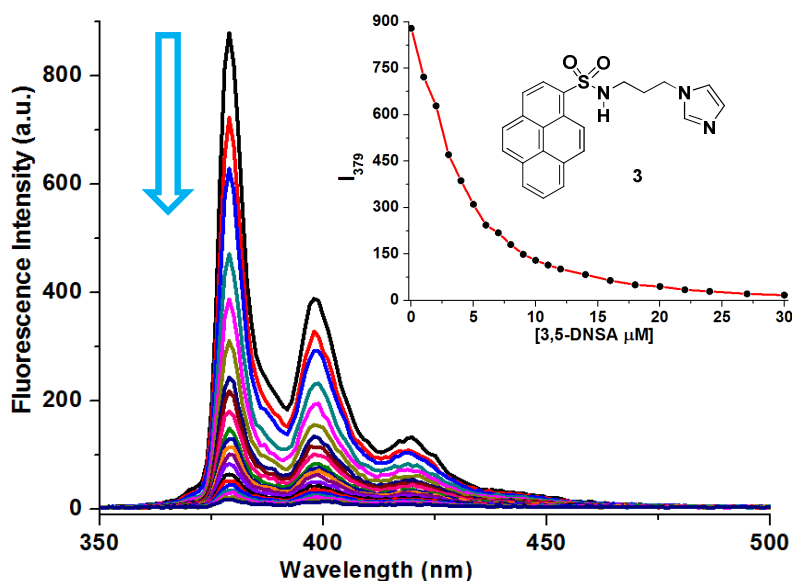


Fig. 5: Fluorescence titration of probe **3** (1 μM in EtOH, $\lambda_{\text{ex}} = 336 \text{ nm}$) with 3,5-dinitrosalicylic acid (inset shows the curve fitting; the filled-in circles show the experimental values and the line is a curve fit).

Fluorescence titration experiments of probe **3** with the acids 3,5-DNSA, 5-NSA, and 5-ISA evidence the formation of 1:1 complexes between probe **3** and the acids, as well as quenching of the pyrene monomer emission intensity. The association constants are listed in Table 1.

Table 1: Association constants ($K_a \text{ (M}^{-1}\text{)}$, in EtOH) of probes **1–5** with various salicylic acid derivatives.

Salicylic acid derivatives	Association constant $K_a \text{ (M}^{-1}\text{)}$ with different probes 1–5				
	1 ^a	2	3	4	5
3,5-DNSA	-----	2.83×10^4	2.66×10^5	7.87×10^3	2.62×10^3
5-NSA	7.18×10^4	9.07×10^3	7.34×10^4	1.87×10^3	1.49×10^3
5-ISA	4.27×10^4	5.32×10^3	4.07×10^4	-----	-----

^aTaken from reference 13b.

Table 1 clearly shows that the imidazole ring in probe **3** results in association constants that are approximately 10 times higher than those measured for probe **2** (and they are similar to those measured for probe **1**). This is probably due to hydrogen bonding of the imidazole C2-H hydrogen with more electronegative oxygens of SA derivatives.

To check, the sulfonamide N-H functionality is more active or less active than the amide N-H functionality with regard to the sensing of SA derivatives, we synthesized probe **4** (which has a C(O)NH group instead of a S(O)₂NH group (probe **3**)). Upon excitation of probe **4** (1 μM in EtOH) at 336 nm, its emission spectrum exhibits monomer fluorescence emission peaks at $\lambda_{\text{max}} = 383$ and 402 nm, with a good quantum yield ($\Phi = 0.160$). Upon the addition of ACAs to a solution of probe **4**, it exhibits behavior that is similar to that of probe **3**, i.e., quenching of the pyrene monomer emission intensity in the order 3,5-DNSA > 5-NSA. However, the degree of quenching of the fluorescence emission intensity is lower (Fig. SI-5). Titration experiments of probe **4** with 3,5-DNSA and 5-NSA evidence the formation of 1:1 complexes between probe **4** and the acids, as well as quenching of the monomer fluorescence emission intensity. The association constants are listed in Table 1.

To understand the role of the sulfonamide N-H functionality, we synthesized probe **5**, which has no N-H and imidazole C2-H functionalities. Upon excitation of probe **5** (1 μM in EtOH) at 336 nm, its emission spectrum exhibits very weak monomer fluorescence emission peaks at $\lambda_{\text{max}} = 379$, 398, and 420 nm, with a low quantum yield ($\Phi = 0.045$). The quantum yield of **5** is approximately 5 times smaller than that of **2**, which has sulfonamide N-H functionality (Figs. 3); this clearly shows the significance of the N-H functionality. Upon the addition of ACAs to the solution of probe **5**, it exhibits a 30% decrease in its emission intensity with 3,5-DNSA and a 10% decrease with 5-NSA; other ACAs did not significantly affect the fluorescence intensity of **5** (Fig. SI-6). Titration experiments of probe **5** with 3,5-

DNSA and 5-NSA evidence the formation of 1:1 complexes between probe **5** and these acids. The association constants, which are rather low, are listed in Table 1.

The studies of the binding of probes **2–5** to ACAs, using the changes in fluorescence, clearly show that probe **5** has a very weak monomer emission and a low quantum yield in comparison with probes **2–4** (Fig. 3), and that **5** undergoes very small changes in the intensity of fluorescence emission upon binding with 3,5-DNSA and 5-NSA (Fig. 6); the association constants are low (Table 1). The change in monomer fluorescence emission intensity of probe **5**, when complexed with 3,5-DNSA, is probably due to hydrogen bonding of the 3,5-DNSA C(O)OH hydroxyl group with the sulfonamide oxygen of probe **5**.

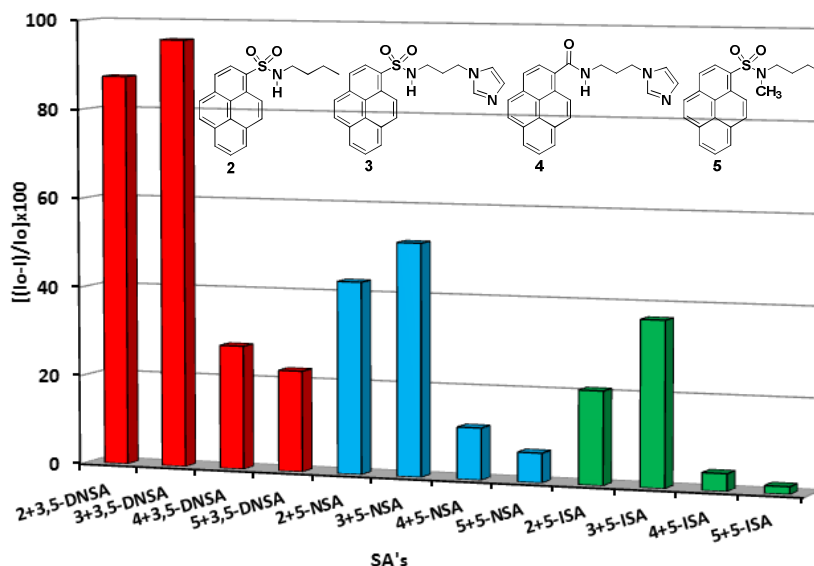


Fig. 6: Bar diagram of the relative fluorescence intensities of probes **2–5** (1 μ M in EtOH, λ_{ex} = 336 nm, λ_{em} = 379 nm) complexed with different SA derivatives (red bars: using 3,5-DNSA; sky-blue bars: using 5-NSA; green bars: using 5-ISA).

To further investigate the nature of the interaction and the mode of complexation of SA derivatives with probes **2–5**, we carried out ^1H NMR titrations of **3**, **4**, and **5** with SA and its derivatives.

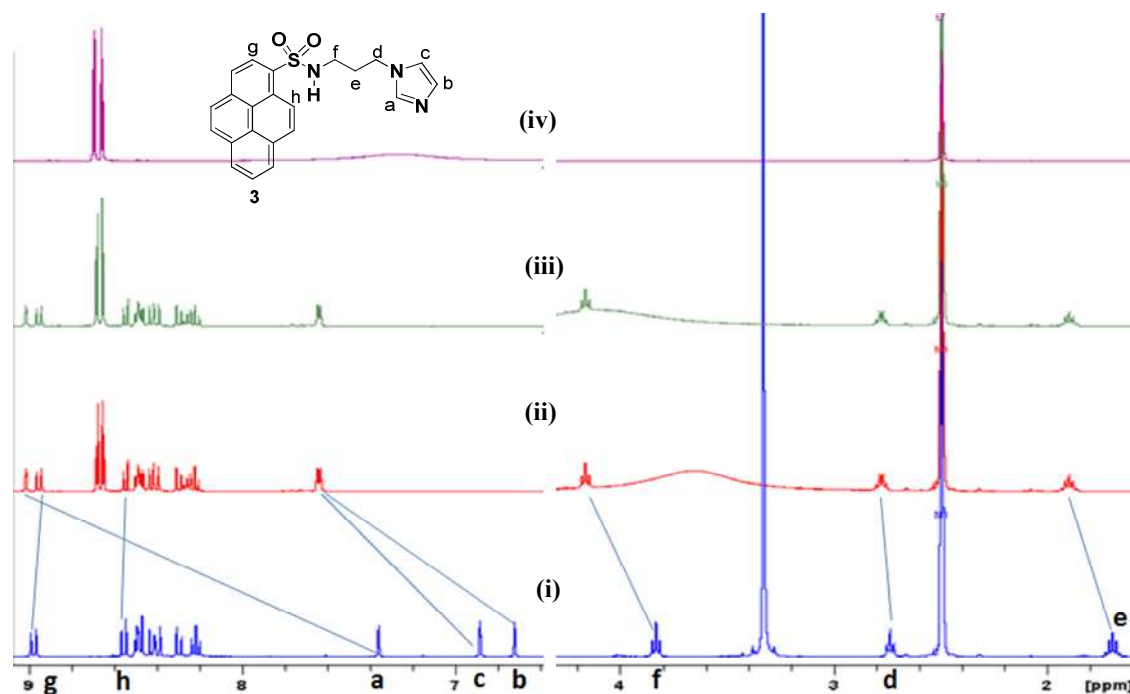


Fig. 7: Partial ^1H NMR spectra ($\text{DMSO-}d_6$) of (i) probe **3**, (ii) **3** + 1 equiv 3,5-DNSA, (iii) **3** + 2 equiv 3,5-DNSA, and (iv) 3,5-DNSA.

The addition of 1 equiv of 3,5-DNSA to a solution of probe **3** in $\text{DMSO-}d_6$ leads to a significant downfield shift of the imidazole C2-H resonance (labeled **a** in Fig. 7) from δ 7.36 to δ 9.01. Signals due to protons **b**, **c**, **d**, **e**, and **f** shift downfield from δ 6.72 to δ 7.63, from δ 6.85 to δ 7.63, from δ 2.73 to δ 2.77, from δ 1.69 to δ 1.89, and from δ 3.83 to δ 4.16, respectively. Additionally, signals due to protons **g** and **h** shift upfield from δ 8.97 to δ 8.94 and from δ 8.55 to δ 8.54, respectively. The addition of 1 more equiv of 3,5-DNSA to this solution does not result in further shifting of the proton signals, which clearly indicates that a 1:1 complex between probe **3** and 3,5-DNSA is formed (Fig. 7). The large changes in the chemical shifts of the labeled protons confirm that both the imidazole C2-H (proton **a**) and the sulfonamide N-H proton (which undergoes exchange with the deuteriums of $\text{DMSO-}d_6$) are involved in hydrogen bonding with 3,5-DNSA. For this reason, the signals due to the aliphatic protons **f** and **e** are shifted more downfield than the signal due to protons **d** (see

Table 2). The upfield shifting of the protons **g** and **h** clearly signifies that the sulfonamide oxygen is also involved in hydrogen bonding.

We also performed the ^1H NMR titration of probe **3** with 3,5-DNSA in CD_3OD ; in this solvent, the signals display shifts similar to those observed in $\text{DMSO-}d_6$ (data obtained in CD_3OD are listed in Table 2). Because of the good solubility of probe **3** in $\text{DMSO-}d_6$, we carried out the titrations with 5-NSA, 5-ISA, and SA in $\text{DMSO-}d_6$; the measured chemical shift differences are listed in Table 2 (Figs. SI-7 – SI-12). The binding behaviors of 5-NSA and 3,5-DNSA were found to be the same.

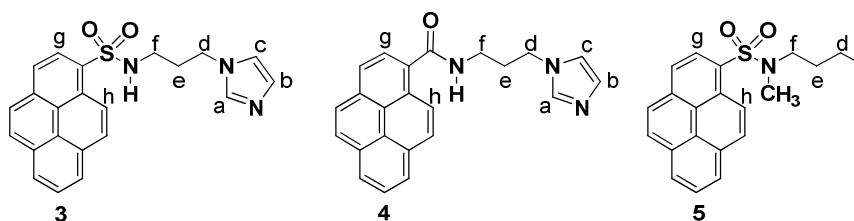


Table 2: Proton chemical shift differences ($\Delta\delta$,^a in $\text{DMSO-}d_6$) measured for probes **3**, **4**, and **5**, induced by the complexation with salicylic acid derivatives.

Probes	3					4	5
	SA	5-ISA	5-NSA	3,5-DNSA	3,5-DNSA ^b	3,5-DNSA	3,5-DNSA
a	0.873	1.467	1.653	1.653	1.500	1.481	NA
b	0.480	0.810	0.910	0.910	0.725	0.819	NA
c	0.430	0.710	0.780	0.780	0.713	0.589	NA
d	0.023	0.038	0.038	0.042	0.022	0.071	
e	0.110	0.181	0.201	0.204	0.226	0.130	
f	0.175	0.280	0.328	0.330	0.410	0.239	
g	-0.012	-0.024	-0.028	-0.035	-0.047	0.040	-0.001
h	-0.003	-0.004	-0.006	-0.010	-0.03	0.020	-0.001

^aPositive values indicate downfield shifting and negative values indicate upfield shifting of the protons in the ^1H NMR spectra upon complexation. ^bMeasured in CD_3OD .

From Table 2 it is clear that 5-ISA causes smaller chemical shift differences than 5-NSA, but larger chemical shift differences than SA. This implies that the strong electron-withdrawing nitro group (NO₂) in 3,5-DNSA and 5-NSA causes these SA derivatives to bind more strongly than 5-ISA (which, in turn, binds more strongly than SA). Hence, the electron-withdrawing group controls the behaviors of the SA derivatives with regard to binding to probe **3**. In the ¹H NMR titration experiments of probe **3** with 5-NSA, 5-ISA, and SA, we found that the proton signals of these acids (i.e., protons **w**, **x**, **y**, and **z**) shift upfield when the acids interact with probe **3** (Figs. SI-7, SI-9 and SI-11). This indicates that these acids accept electron charge from the electron-rich pyrene ring of probe **3** through charge transfer. This is also supported by the decay time of probe **3** and its complex with 3,5-DNSA that shows only slight difference in the decay time as compared with 3,5-DNBA (Figs. SI-13 and SI-14). So the formation of [**3**•3,5-DNSA]-complex occurs in the ground state that overrules the possibility of PET phenomenon. With regard to probe **4**, the addition of 1 equiv of 3,5-DNSA causes downfield shifting of all of the proton signals (**a–h**); the addition of one extra equiv of 3,5-DNSA does not cause any further downfield shifting (Figs. SI-15 and SI-16). This confirms the formation of a 1:1 complex between probe **4** and 3,5-DNSA. Hence, 3,5-DNSA probably binds probe **3** in the same way that it binds probe **4**. The addition of 1 equiv of 3,5-DNSA to a DMSO-*d*₆ solution of probe **5** leaves most of the proton signals unaffected, although protons **g** and **h** of the pyrene ring do show some upfield shifting (Figs. SI-17 and SI-18). This could be due to hydrogen bonding of the salicylic acid, i.e. OH of the COOH with sulfonamide oxygen.

To understand the mechanism of the interaction of SA derivatives with probe **3**, we performed energy-minimization calculations using gradient-correlated density functional theory (DFT). The optimized structures of the complexes **3**•3,5-DNSA and **3**•5-NSA are presented in Fig. 8. The binding energies of 5-NSA and 3,5-DNSA with probe **3** are 7.3 and

14.3 kcal/mol, respectively, showing that probe **3** has a higher tendency to bind 3,5-DNSA than to bind 5-NSA. This agrees with our experiments, in which we found that 3,5-DNSA has the higher association constant (Table 1). The complex **3**•3,5-DNSA is 7.0 kcal/mol more stable than the complex **3**•5-NSA, which is due to the additional strong hydrogen bond between the OH and NO₂ groups in 3,5-DNSA.

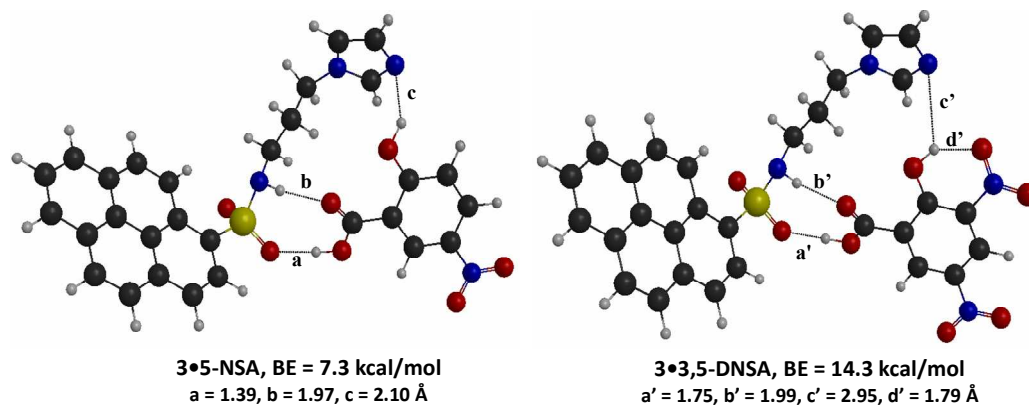


Fig. 8: Energy-minimized geometries of complexes of probe **3** with 5-NSA and 3,5-DNSA, calculated by B3LYP/6-31G*.

The electronic transitions are predominantly characterized by HOMO \rightarrow LUMO at the excited-state geometry. We find that binding of 5-NSA and 3,5-DNSA to **3** results in a decrease of the HOMO-LUMO energy difference; the decrease is more pronounced with 3,5-DNSA than with 5-NSA, which leads to strong binding between 3,5-DNSA and probe **3** (Figs. 9, SI-19, and SI-20, and Table SI-1). Using B3LYP/6-31G*, the fluorescence emission spectra of probe **3** and its complexes with 5-NSA and 3,5-DNSA were obtained (they are shown in Fig. SI-21). The calculated spectra also support the experiment results, i.e., the quenching of fluorescence intensity of probe **3** is higher with 3,5-DNSA than with 5-NSA, which leads to a higher association constant. We have also found that probe **3** can be used for the detection of 3,5-DNSA over a wide pH range between 3-12 (Fig. SI 22).

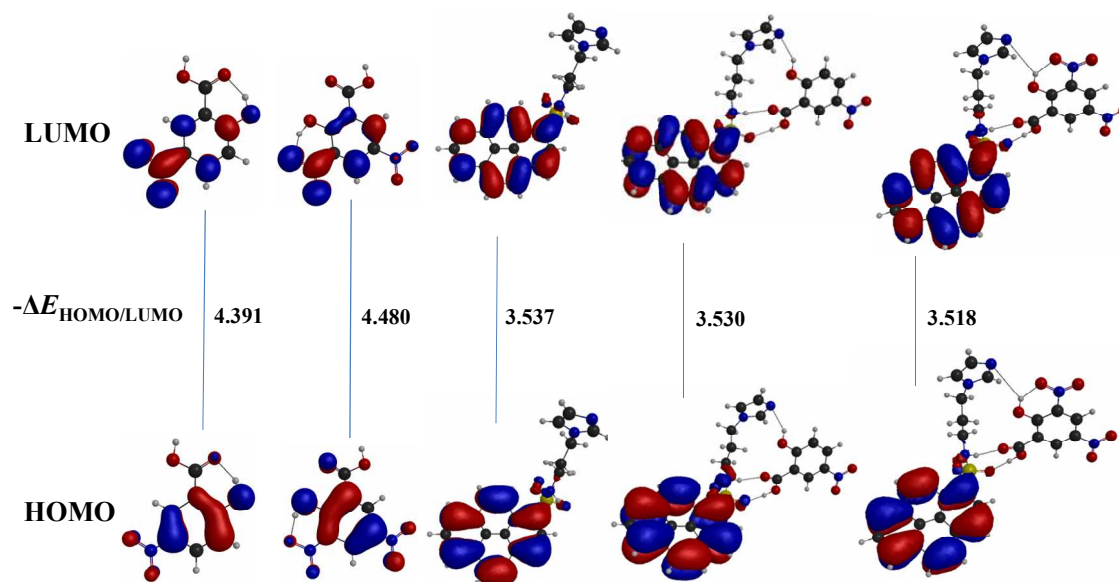


Fig. 9: Calculated (B3LYP/6-31G*) molecular orbitals of 5-NSA, 3,5-DNSA, probe 3, and complexes of probe 3 with 5-NSA and 3,5-DNSA.

3. Conclusions

In conclusion, this is the first report in which simple pyrenesulfonamides have been used for the recognition of SA derivatives. Probes 2 and 3 both have a sulfonamide N-H functionality as a hydrogen bonding motif (which plays a crucial role), and the presence of the C2-H group in the imidazole ring in probe 3 provides the additional hydrogen bonding site that holds the SA in close proximity to the pyrene ring. This results in a high association constant for 3,5-DNSA and in complete quenching of the fluorescence emission intensity due to charge transfer from the pyrene unit to the electron-deficient aromatic ring of 3,5-DNSA. ^1H NMR titration experiments and DFT calculations clearly support the mechanism with which the probes interact with SA and SA derivatives.

4. Experimental section

4.1. General

Melting points were determined using a Thomas-Hoover capillary melting point apparatus and are uncorrected. ^1H and ^{13}C NMR spectra were recorded on a Bruker AM-400 spectrometer, using Me_4Si as the internal standard. FAB mass spectrometry was performed at the KBSI Daegu branch. UV-visible absorption spectra were recorded on a Shimadzu UV-1650PC spectrophotometer. Fluorescence spectra were measured on a Shimadzu RF-5301 fluorescence spectrometer equipped with a xenon discharge lamp, 1 cm quartz cells and with slit width 3 nm. The fitting of the fluorescence titration data was done using gunplot 4.6 software. All of the measurements were performed at 298 K. Analytical grade ethanol was purchased from Merck. All other materials for syntheses were purchased from Aldrich Chemical Co. and they were used as received. Quantum yields (Φ) were determined using the procedure reported in the literature.¹⁹

4.2. Theoretical calculations

The geometries of all compounds were optimized using gradient-correlated density functional theory (DFT) using the Becke three-parameter exchange functional²⁰ and the Lee-Yang-Parr correlation functional (B3LYP).²¹ All-electron 6-31G(d,p) basis sets were used. Time-dependent density functional theory (TD-DFT) was used for excited-state calculations. The fluorescence emission spectra were plotted using excitation and oscillator strength of the molecule in TD-DFT calculations. TD-B3LYP/6-31G(d,p) calculations were used for excited-state optimizations of 5-NSA, 3,5-DNSA, probe **3**, and for SA complexes of **3**. All of the calculations herein were performed with GAMESS (General Atomic and Molecular Electronic Structure System).²²

4.3. Syntheses of probes 2–5

4.3.1. Pyrene-1-butyl-sulfonamide (probe **2**)

To a solution of pyrenesulfonic acid (500 mg, 1.8 mmol) in *N,N*-dimethylformamide (10 mL) was added thionyl chloride (0.785 mL, 6 mmol), and the mixture was subsequently stirred for

3 h at 0 °C under an argon atmosphere. After the reaction had completed, the reaction mixture was poured onto ice. The yellow precipitate was filtered and washed with water. The solid was dried for 12 h at 50 °C. The required pyrenesulfonyl chloride was further purified by column chromatography, using CH₂Cl₂ as the eluent ($R_f = 0.85$), and it was obtained in a yield of 70% (373 mg). Melting point: 169 °C. The pyrenesulfonyl chloride was used for further reactions. A solution of pyrenesulfonyl chloride (300 mg, 1.0 mmol) in CH₂Cl₂ (22 mL) was added dropwise to a stirred solution of *n*-butylamine (220 mg, 3 mmol) in CH₂Cl₂ (5 mL) at 0 °C under an argon atmosphere. The reaction mixture was subsequently stirred at room temperature for another 2 h. The CH₂Cl₂ layer was washed with H₂O (2 × 50 mL) and with 100 mL of an aqueous solution of NaCl (5%), dried over anhydrous sodium sulfate, and filtered. The filtrate was evaporated under reduced pressure and the residue was purified by column chromatography, using CH₂Cl₂ as the eluent ($R_f = 0.50$), to give **2** as a light yellow solid (233 mg, 69% yield). Melting point: 115 °C (CH₂Cl₂/hexane). ¹H NMR (400 MHz, CDCl₃) δ 0.73 (t, $J = 7.3$ Hz, 3H, CH₃), 1.17–1.22 (m, 2H, CH₂), 1.35–1.39 (m, 2H, CH₂), 2.94 (t, $J = 7.1$ Hz, 2H, CH₂), 4.73 (bs, 1H, NH), 8.12–8.16 (m, 2H, 2 × ArH), 8.25 (d, $J = 8.6$ Hz, 1H, ArH), 8.32–8.37 (m, 3H, 3 × ArH), 8.73 (d, $J = 8.4$ Hz, 1H, ArH), 9.01 (d, $J = 9.4$ Hz, 1H, ArH). ¹³C NMR (100 MHz, CDCl₃) δ 13.81 (CH₃), 20.00 (CH₂), 31.96 (CH₂), 43.44 (CH₂), 123.44, 124.26, 124.44, 125.60, 127.20, 127.29, 127.39, 127.46, 127.89, 128.41, 130.52, 130.53, 130.56, 131.31, 131.52, 135.20. HR-mass calcd for C₂₀H₁₉NO₂S (M⁺): 337.1136; found: m/z 337.1141.

4.3.2. Pyrene-1-(3-imidazol-1-yl-propyl)-sulfonamide (probe **3**)

Probe **3** was prepared according to the literature procedure.^{14q} To a solution of 1-(3-aminopropyl)imidazole (250 mg, 2 mmol) in CH₂Cl₂ (5 mL) was added a solution of pyrenesulfonyl chloride (373 mg, 1.24 mmol) dissolved in CH₂Cl₂ (25 mL) at 0 °C under an argon atmosphere. The reaction mixture was subsequently stirred at room temperature for

another 2 h. The CH₂Cl₂ layer was washed with H₂O (2 × 50 mL) and with 100 mL of an aqueous solution of NaCl (5%), dried over anhydrous sodium sulfate, and filtered. The filtrate was evaporated under reduced pressure and the residue was purified by column chromatography, using CH₂Cl₂/CH₃OH (9:1) as the eluent ($R_f = 0.15$), to give **3** as a light yellow solid (344 mg, 71% yield). Melting point: 200 °C (CH₂Cl₂/hexane). ¹H NMR (400 MHz, DMSO-*d*₆) δ 1.68–1.72 (m, 2H, CH₂), 2.73–2.75 (m, 2H, CH₂), 3.84 (t, $J = 6.8$ Hz, 2H, CH₂), 6.72 (s, 1H, ArH), 6.85 (s, 1H, ArH), 7.36 (s, 1H, ArH), 8.23 (t, $J = 7.6$ Hz, 1H, ArH), 8.31 (d, $J = 9.1$ Hz, 1H, ArH), 8.41 (d, $J = 8.8$ Hz, 1H, ArH), 8.44 (d, $J = 8.3$ Hz, 1H, ArH), 8.48–8.51 (m, 3H, 3 × ArH), 8.57 (d, $J = 8.1$ Hz, 1H, ArH), 8.99 (d, $J = 9.4$ Hz, 1H, ArH). ¹³C NMR (100 MHz, DMSO-*d*₆) δ 31.07 (CH₂), 43.38 (CH₂), 119.43, 123.54, 123.63, 124.64, 124.66, 127.14, 127.26, 127.46, 127.49, 127.57, 128.62, 129.97, 130.04, 130.39, 130.90, 132.52, 134.39, 137.40. HR-FAB mass calcd for C₂₂H₁₉N₃O₂S ([M+H]⁺): 390.1276; found: m/z 390.1273.

4.3.3. Pyrene-1-(3-imidazol-1-yl-propyl)-amide (probe **4**).

At room temperature, thionyl chloride (4 mL, 30 mmol) was added dropwise, over a period of 30 min, to a solution of pyrenecarboxylic acid (492 mg, 2 mmol) in CH₂Cl₂ (10 mL), and the mixture was subsequently stirred for 3 h at 60 °C under an argon atmosphere. After completion of the reaction, the solvent was removed under vacuum. 1-(3-Aminopropyl)imidazole (250 mg, 2 mmol) was added to the resulting residue in dry CH₂Cl₂ (10 mL) at room temperature. The reaction mixture was stirred for 5 h at 70 °C under an argon atmosphere. After completion of the reaction, the reaction mixture was concentrated and purified by column chromatography, using CH₂Cl₂/CH₃OH (9:1) as the eluent ($R_f = 0.10$), to give **4** as a white solid (280 mg, 71%). Melting point: 151 °C (CH₂Cl₂/hexane). ¹H NMR (400 MHz, DMSO-*d*₆) δ 2.03–2.10 (m, 2H, CH₂), 3.36–3.39 (m, 2H, CH₂), 4.13 (t, $J = 6.8$ Hz, 2H, CH₂), 6.92 (s, 1H, ArH), 7.27 (s, 1H, ArH), 7.72 (s, 1H, ArH), 8.12–8.16 (m, 2H, 2 ×

ArH), 8.21–8.27 (m, 3H, 3 × ArH), 8.33–8.36 (m, 2H, 2 × ArH), 8.48 (d, $J = 9.2$ Hz, 1H, ArH), 8.79 (t, $J = 8.1$ Hz, 1H, ArH). ^{13}C NMR (100 MHz, DMSO- d_6) δ 31.20 (CH₂), 37.00 (CH₂), 44.22 (CH₂), 119.84, 124.01, 124.16, 124.78, 125.02, 125.66, 125.99, 126.19, 126.97, 127.59, 128.13, 128.52, 128.65, 128.74, 130.57, 131.09, 131.95, 132.31, 137.76, 169.41 (C=O). HR-FAB mass calcd for C₂₃H₂₀N₃O ([M+H]⁺): 354.1606; found: m/z 354.1610.

4.2.3. Pyrene-1-butyl-1'-methyl-sulfonamide (probe 5)

A solution of pyrenesulfonyl chloride (300 mg, 1.0 mmol) in CH₂Cl₂ (22 mL) was added dropwise to a solution of *N*-methylbutylamine (262 mg, 3 mmol) in CH₂Cl₂ (5 mL) at 0 °C under an argon atmosphere. The reaction mixture was subsequently stirred at room temperature for another 2 h. The CH₂Cl₂ layer was washed with H₂O (2 × 50 mL) and with 100 mL of an aqueous solution of NaCl (5%), dried over anhydrous sodium sulfate, and filtered. The filtrate was evaporated under reduced pressure and the residue was purified by column chromatography, using CH₂Cl₂ as the eluent ($R_f = 0.80$), to give **5** as a light yellow solid (320 mg, 95%). Melting point: 130 °C (CH₂Cl₂/hexane). ^1H NMR (400 MHz, CDCl₃) δ 0.77 (t, $J = 7.2$ Hz, 3H, CH₃), 1.18–1.24 (m, 2H, CH₂), 1.42–1.46 (m, 2H, CH₂), 2.80 (s, 3H, NCH₃), 3.17 (t, $J = 7.2$ Hz, 2H, CH₂), 8.21 (t, $J = 7.6$ Hz, 1H, ArH), 8.31 (d, $J = 9.2$ Hz, 1H, ArH), 8.41 (d, $J = 8.8$ Hz, 1H, ArH), 8.44–8.49 (m, 4H, 4 × ArH), 8.54 (d, $J = 8.4$ Hz, 1H, ArH), 8.97 (d, $J = 9.2$ Hz, 1H, ArH). ^{13}C NMR (100 MHz, CDCl₃) δ 14.05 (CH₃), 20.12 (CH₂), 30.05 (CH₂), 34.54 (CH₃), 49.86 (CH₂), 124.24, 124.29, 124.36, 125.64, 127.09, 127.14, 127.23, 127.38, 128.12, 129.10, 130.03, 130.52, 130.76, 131.32, 135.04. HR-mass calcd for C₂₁H₂₂NO₂S ([M+H]⁺): 352.1371; found: m/z 352.1375.

Acknowledgment

This research was supported by the Basic Science Research Program through the National Research Foundation of Korea (NRF), which is funded by the Ministry of Science, ICT, and Future Planning (2013R1A1A2006777). H.Kim thanks professor Taiha Joo at POSTECH for

valuable discussion and decay time experiment.

References

1. (a) L. Styrer, *Biochemistry*, W. H. Freeman, New York, 3rd Edn., pp. 188, 373–394, 376 and 575; (b) M. Afran, H. R. Athar and M. Ashar, *J. Plant Physiol.*, 2007, **164**, 685.
2. M. S. Maynor, T. L. Nelson, C. O'Sullivan and J. J. Lavigne, *Org. Lett.*, 2007, **9**, 3217.
3. A. T. Gates, S. O. Fakayode, M. Lowry, G. M. Ganea, A. Murugesu, J. W. Robinson, R. M. Strongin and I. M. Warner, *Langmuir*, 2008, **24**, 4107.
4. V. Adam, J. Zehnalek, J. Petrlova, D. Potesil, B. Sures, L. Trnkova, F. Jelen, J. Vitecek and R. Kizek, *Sensors*, 2005, **5**, 70.
5. D. James, S. M. Scott, Z. Ali and W. T. O'Hare, *Microchim. Acta*, 2005, **149**, 1.
6. (a) K. Ghosh, T. Sen and R. Frohlich, *Tetrahedron Lett.*, 2007, **48**, 7022; (b) A. K. Mahapatra, P. Sahoo, S. Goswami and H.-K. Fun, *J. Lumin.*, 2011, **131**, 59; (c) M. Lee, H. Zali-Boeini, F. Li, L. F. Lindoy and K. A. Jolliffe, *Tetrahedron*, 2013, **69**, 38; (d) X. Yang, X. Liu, K. Shen, Y. Fu, M. Zhang, C. Zhu and Y. Cheng, *Org. Biomol. Chem.*, 2011, **9**, 6011.
7. M. W. Ahmad, S. H. Kim, and H.-S. Kim, *Tetrahedron Lett.*, 2011, **52**, 6743.
8. (a) S. Goswami, S. Jana, S. Dey, D. Sen, H.-K. Fun, and S. Chantrapromma, *Tetrahedron*, 2008, **64**, 6426; (b) A. I. Oliva, L. Simon, F.M. Muniz, F. Sanz and J. R. Moran, *Tetrahedron*, 2004, **60**, 3755.
9. (a) G. Moore, C. Papamicael, V. Levacher, J. Bourguignon and G. Dupas, *Tetrahedron*, 2004, **60**, 4197; (b) M. Almaraz, M. Martin, J. V. Hernandez, M. C. Caballero and J. R. Moran, *Tetrahedron Lett.*, 1998, **39**, 1811.

-
10. (a) S. J. Geih, C. Vicent, E. Fan, and A. D. Hamilton, *Angew. Chem., Int. Ed.*, 1993, **32**, 119; (b) S. Goswami, K. Ghosh, and M. Halder, *Tetrahedron Lett.*, 1999, **40**, 1735; (c) S. Goswami, A. Hazra, and H.-K. Fun, *J. Incl. Phenom. Macrocycl. Chem.*, 2010, **68**, 461; (d) S. Goswami, N. K. Das, D. Sen, and H.-K. Fun, *Supramolecular Chem.*, 2010, **22**, 532; (e) K. Ghosh, G. Masanta, R. Frohlich, I. D. Petsalakis, and G. Theodorakopoulos, *J. Phys. Chem. B*, 2009, **113**, 7800; (f) K. Ghosh, T. Sen and R. Frohlich, *Tetrahedron Lett.*, 2007, **48**, 2935.
11. (a) S. Goswami, N. K. Das, D. Sen, G. Hazra, J. H. Goh, Y. C. Sing, and H.-K. Fun, *New J. Chem.*, 2011, **35**, 2811; (b) M. L. Mussons, C. Raposo, J. Anaya, M. Grande, J. R. Moran and M. C. Caballero, *J. Chem. Soc. Perkin Trans.* 1992, **1**, 3125; (c) S. Goswami, K. Ghosh, and S. Dasgupta, *J. Org. Chem.*, 2000, **65**, 1907; (d) G. Moore, V. Levacher, J. Bourguignon and G. Dupas, *Tetrahedron Lett.*, 2001, **42**, 261.
12. (a) H.-C. Chou, C.-H. Hsu, Y.-M. Cheng, C.-C. Cheng, H.-W. Liu, S.-C. Pu and P.-T. Chou, *J. Am. Chem. Soc.*, 2004, **126**, 1650; (b) K. Uzarevic, I. Halasz, I. Dilovic, N. Bregovic, M. Rubcic, D. Matkovic-C alogovic and V. Tomisic, *Angew. Chem., Int. Ed.*, 2013, **52**, 5504; (c) K. Ghosh, I. Saha, G. Masanta, E. B. Wang and C. A. Parish, *Tetrahedron Lett.*, 2010, **51**, 343; (d) S. Zakavi, M. N. Ragheb and M. Rafiee, *Inorg. Chem Commun.*, 2012, **22**, 48; (e) T. Kusukawa, K. Toyama, S. Takeshita and S. Tanaka, *Tetrahedron*, 2012, **68**, 9973; (f) P. Saliuga, N. Kaur, J. Kang, N. Singh and D. O. Jang, *Tetrahedron*, 2013, **69**, 9001; (g) S. Goswami, K. Ghosh and R. Mukherjee, *Tetrahedron*, 2001, **57**, 4987; (h) T. Moriuchi, K. Yoshida and T. Hirao, *Org. Lett.*, 2003, **5**, 4285; (i) S. Goswami, S. Dey, H.-K. Fun, S. Anjum and A.-U. Rahman, *Tetrahedron Lett.*, 2005, **46**, 7187; (j) S. Goswami, S. Jana, S.Dey, I. A. Razak and H.-K. Fun, *Supramol. Chem.*, 2006, **18**, 571; (k) S. Goswami, S. Jana and H.-K. Fun, *CrystEngComm*, 2008, **10**, 507; (l) C. B. Aakeroy, J. Desper, B. Leonard and J. F. Urbina, *Cryst. Growth Des.*, 2005, **5**, 865; (m) J. R. Jadhav, M. W. Ahmad and H.-S. Kim, *Tetrahedron Lett.*, 2010, **51**, 5954.

-
13. (a) J. Yoon, J. R. Jadhav, J. M. Kim, M. Cheong, H.-S. Kim and J. Kim, *Chem. Commun.*, 2014, **50**, 7670; (b) M. W. Ahmad, B.-Y. Kim and H.-S. Kim, *New J. Chem.*, 2014, **38**, 1711.
14. (a) D. Elbaum, S. K. Nair, M. W. Patchan, R. B. Thompson, and D. W. Christianson, *J. Am. Chem. Soc.* 1996, **118**, 8381; (b) J. T. Suri, D. B. Cordes, F. E. Cappuccio, R. A. Wessling, and B. Singaram, *Angew. Chem. Int. Ed.*, 2003, **42**, 5857; (c) T. W. Kim, J.-H. Park and J.-I. Hong, *J. Chem. Soc., Perkin Trans.* 2002, **2**, 923; (d) Y. M. Chung, B. Raman, D.-S. Kim and K. H. Ahn, *Chem. Commun.*, 2006, 186; (e) M. T. Huggins, T. Butler, P. Barber and J. Hunt, *Chem. Commun.*, 2009, 5254; (f) W. Jiang, Y. Cao, Y. Liu and W. Wang, *Chem. Commun.*, 2010, **46**, 1944; (g) C. N. Carroll, B. A. Coombs, S. P. McClintock, C. A. Johnson II, O. B. Berryman, D. W. Johnson and M. M. Haley, *Chem. Commun.*, 2011, **47**, 5539; (h) J.-M. Kim, C. R. Lohani, L. N. Neupane, Y. Choi and K.-H. Lee, *Chem. Commun.*, 2012, **48**, 3012; (i) H. Aboubakr, H. Brisset, O. Siri, and J.-M. Raimundo, *Anal. Chem.*, 2013, **85**, 9968; (j) N. Laurieri, M. H. J. Crawford, A. Kawamura, I. M. Westwood, J. Robinson, A. M. Fletcher, S. G. Davies, E. Sim, and A. J. Russell, *J. Am. Chem. Soc.*, 2010, **132**, 3238; (k) J. Yin, Y. Kwon, D. Kim, D. Lee, G. Kim, Y. Hu, J.-H. Ryu, and J. Yoon, *J. Am. Chem. Soc.*, 2014, **136**, 5351; (l) R. Sakai, E. B. Barasa, N. Sakai, S.-I. Sato, T. Satoh, and T. Kakuchi, *Macromolecules*, 2012, **45**, 8221; (m) V. Luxami, A. S. Gupta and K. Paul, *New J. Chem.*, 2014, **38**, 2841; (n) N. V. Ghule, S. V. Bhosale and S. V. Bhosale, *RSC Adv.*, 2014, **4**, 27112; (o) Y. Cao, L. Ding, S. Wang, Y. Liu, J. Fan, W. Hu, P. Liu, and Y. Fang, *ACS Appl. Mater. Interfaces*, 2014, **6**, 49; (p) T. Ema, K. Okuda, S. Watanabe, T. Yamasaki, T. Minami, N. A. Esipenko, and P. Anzenbacher, *Org. Lett.*, 2014, **16**, 1302; (q) A. Kumar and H.-S. Kim, *New J. Chem.*, 2015, DOI: 10.1039/c4nj01603c.
15. (a) M.-H. Yang, P. Thirupathi, and K.-H. Lee, *Org. Lett.*, 2011, **13**, 5028; (b) L. N. Neupane, J.-Y. Park, J. H. Park, and K.-H. Lee, *Org. Lett.*, 2013, **15**, 254; (c) H. J. Kim, J. Hong, A. Hong, S. Ham, J. H. Lee, and J. S. Kim., *Org. Lett.*, 2008, **10**, 1963; (d) S. Jang, P. Thirupathi, L. N. Neupane, J. Seong, H. Lee, W. I. Lee, and K.-H. Lee, *Org. Lett.*, 2012, **14**, 4746.

-
16. (a) N. Yan, Z. Xu, K. K. Diehn, S. R. Raghavan, Y. Fang, and R. G. Weiss, *J. Am. Chem. Soc.*, 2013, **135**, 8989; (b) N. Yan, Z. Xu, K. K. Diehn, S. R. Raghavan, Y. Fang, and R. G. Weiss, *Langmuir*, 2013, **29**, 793–805.
17. K. Zhao, T. Liu, G. Wang, X. Chang, D. Xue, K. D. Belfield, and Y. Fang, *J. Phys. Chem. B*, 2013, **117**, 5659–5667.
18. (a) J. Yoon, S. K. Kim, N. J. Singh and K. S. Kim, *Chem. Soc. Rev.*, 2006, **35**, 355; (b) S. Kumar, V. Luxami, and A. Kumar, *Org. Lett.*, 2008, **10**, 5549; (c) Z. Xu, S. K. Kim and J. Yoon, *Chem. Soc. Rev.*, 2010, **39**, 1457; (d) F. Zapata, A. Caballero, N. G. White, T. D. W. Claridge, P. J. Costa, Vitor Felix, and P. D. Beer, *J. Am. Chem. Soc.*, 2012, **134**, 11533; (e) E. Faggi, R. Porcar, M. Bolte, S. V. Luis, E. Garcia-Verdugo, and I. Alfonso, *J. Org. Chem.*, 2014, **79**, 9141; (f) J. Cai and J. L. Sessler, *Chem. Soc. Rev.*, 2014, **43**, 6198; (g) C. Gao, G. Gao, J. Lan and J. You, *Chem. Commun.*, 2014, **50**, 5623; (h) J. R. Jadhav, M. W. Ahmad, and H.-S. Kim, *Bull. Korean Chem. Soc.*, 2011, **32**, 2933.
19. A. Kumar, V. Vanita, A. Walia, and S. Kumar, *Sens. Actuator B Chem.* 2013, **177**, 904.
20. A. D. Becke, *J. Chem. Phys.*, 1993, **98**, 5648.
21. C. Lee, W. Yang, and R. G. Parr, *Phys. Rev. B: Condens. Matter*, 1988, **37**, 785.
22. M. W. Schmidt, K. K. Balbridge, J. A. Boatz, S. T. Elbert, M. S. Gordon, J. H. Jensen, S. Koseki, N. Matsunaga, K. A. Nguyen, S. Su, T. L. Windus, M. Dupuis, and J. A. J. Montgomery, *J. Comput. Chem.*, 1993, **14**, 1347.